Chinese Chemical Letters 33 (2022) 1288–1292

Contents lists available at ScienceDirect

Chinese Chemical Letters

journal homepage: www.elsevier.com/locate/cclet

Embedding wasted hairs in Ti/PbO_2 anode for efficient and sustainable electrochemical oxidation of organic wastewater

Dan Shao[a,*], Zekang Wang[a], Cuiping Zhang[a], Weijia Li[a], Hao Xu[b,*], Guoqiang Tan[a], Wei Yan[b]

[a] School of Materials Science and Engineering, Shaanxi Key Laboratory of Green Preparation and Functionalization for Inorganic Materials, Shaanxi University of Science & Technology, Xi'an 710021, China
[b] Department of Environmental Engineering, Xi'an Jiaotong University Xi'an, 710049, China

ARTICLE INFO

Article history:
Received 14 April 2021
Revised 25 July 2021
Accepted 27 July 2021
Available online 31 July 2021

Keywords:
Wastewater treatment
Lead dioxide
Fiber
Composite
Intermediate product

ABSTRACT

Despite of the hazardous risk of Pb^{2+} leakage, lead dioxide has been attributed as a quasi-ideal anode material with high oxygen evolution potential, excellent conductivity, good stability and low cost in electrochemical oxidation wastewater treatment technique. In this study, a novel Ti/PbO_2 anode was fabricated by embedding raw materials that are readily and cheaply available, *i.e.*, hairs. The structure-activity relationship of the new electrode was firstly revealed by material and electrochemical characterizations. Then different levels of pollutants (azo dye, phenol and maleic acid) were used to investigate the electrochemical oxidation performance of the new electrode. Finally, the accelerated electrode lifetime and Pb^{2+} leakage tests were carried out. Results showed that the embedded hairs changed the preferential crystallographic orientation of PbO_2 and decreased the grain size. Hairs introduced additional roughness and active sites, and decreased the electrode impedance, especially under 5 mg/cm^2 of embedding amount. The removal efficiencies of different target pollutants were enhanced more or less by embedding appropriate amount of hairs, depending on the current density, but loading excessive hairs had a negative effect. The accumulation of intermediate products during phenol degradation was also changed by the hairs. The new electrode could undergo ~550 h of harsh electrolysis. It is also relieved that the Pb^{2+} leakage was found to be suppressed during this long-term electrolysis process.

Electrochemical oxidation wastewater treatment (EOWT) has merits of forcible oxidation ability, clean agent, low equipment requirement, high mobility and easy automation. EOWT is attributed as one of the most promising techniques to complement biotreatment and other physical and chemical methods, especially when handling nonbiodegradable, toxic or refractory organic pollutants [1-5]. Anode material plays a crucial role in EOWT because it offers the main oxidizing reaction location and suffers the highly corrosive environment [6-10]. The prerequisite of a proper anode material is the high oxygen evolution potential (OEP), because the oxygen evolution reaction (OER) is the main side reaction [11-14]. Boron-doped diamond (BDD), titanium black (Ti_4O_7), antimony doped tin dioxide (Sb-SnO_2) and lead dioxide (PbO_2) are four typical high OEP anode materials. The PbO_2 (usually Ti/PbO_2) has been attributed as a competitive anode material among the above four anodes with excellent conductivity, good stability and low cost [15,16].

Despites of these merits, the fear of Pb^{2+} leakage in certain scenarios (*e.g.*, drinking water), poor toughness, and the limited surface area confines the application of PbO_2 anode [17-19]. Doping ions (*e.g.*, F^-, Fe^{3+}, Cu^{2+} and rare earths), compositing second phase materials (*e.g.*, TiO_2 particles, PTFE, and nano fibers), introducing various interlayers (*e.g.*, Sb-SnO_2 interlayer), and constructing porous coating structures are four main Ti/PbO_2 modification approaches [20-26]. However, these approaches either have limitations, or use more chemicals, or increase preparation difficulty (or cost) significantly.

In this study, hairs, readily and cheaply available raw materials, were facilely embedded into the PbO_2 layer to form a brand-new Ti/PbO_2. At first, the PbO_2 layer were expected to be toughen by this approach. But when study went deeper, it was found that hairs also enhanced the pollutant removal efficiency, as well as the electrode's environmental friendliness. The morphology, composition and structure of the new electrode were firstly examined.

* Corresponding authors.
E-mail addresses: shaodan@sust.edu.cn (D. Shao), xuhao@mail.xjtu.edu.cn (H. Xu).

https://doi.org/10.1016/j.cclet.2021.07.061
1001-8417/

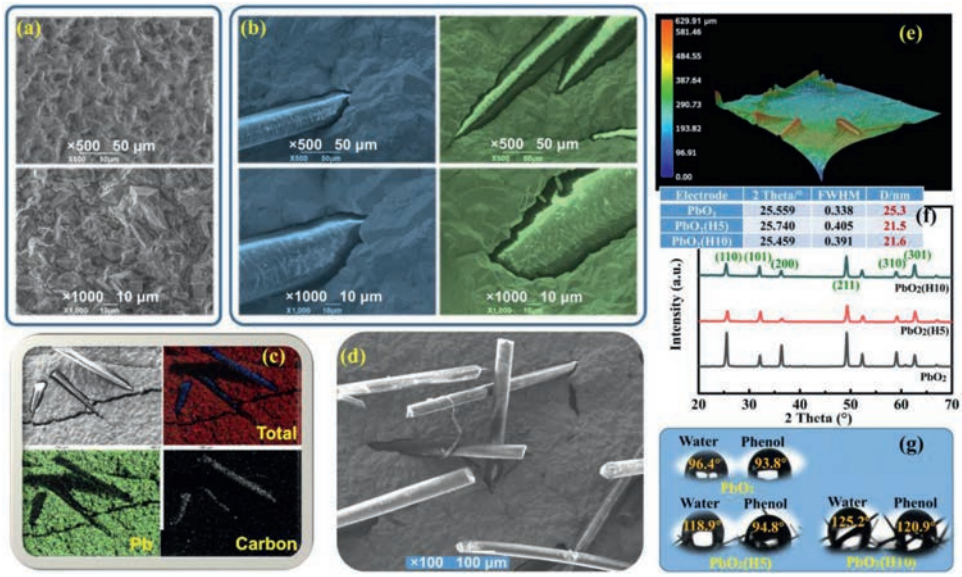

Fig. 1. Material characterization results of the hair-embedded anodes and the unmodified anode: (a) SEM images of PbO_2; (b) SEM images of PbO_2(H5) and PbO_2(H10); (c) EDS mappings of a part of PbO_2(H5); (d) SEM images of a part of PbO_2(H5); (e) 3D microscopic images of a part of PbO_2(H5); (f) XRD patterns (The table refers to gain sizes (D values) calculated from different full widths at half-maximum (FWHM) of (110) facet peaks by Scherrer equation.); (g) Contact angles towards water and phenol.

Then necessary electrochemical characterizations were performed. Furtherly, three model compounds, azo dye acid red G (ARG), phenol and maleic acid were used as the target pollutants to test the comprehensive oxidation ability of the new electrode. This study was expected to offer a cost-effective, robust and green Ti/PbO_2 anode for EWOT.

Ti plate (99.9%, 3 cm × 4 cm) was pretreated and loaded with TiH_x and Sb-SnO_2 interlayers as reported [27]. Then PbO_2 coating was electrodeposited on these interlayers. The electrodeposition solution was 0.25 L pure water (18.2 MΩ cm) containing 41.407 g $Pb(NO_3)_2$, 6.042 g $Cu(NO_3)_2$, and 0.105 g NaF. A certain amount of hairs were dispersed in this solution. During the 60 min of electrodeposition, the solution was heated (65 °C) and stirred. The anodic current density was 15 mA/cm^2. The prepared Ti/TiH_x/Sb-SnO_2/PbO_2 anode without hairs was named as PbO_2 briefly, and the anodes with ~5 mg/cm^2 and ~10 mg/cm^2 of embedded hairs were named as PbO_2(H5) and PbO_2(H10), respectively. The characterization details are described in Supporting information. The degradation experiments were carried out in a standard two-electrode cell at room temperature. Chemical pure ARG, phenol and maleic acid were dissolved in 0.25 L of pure water, respectively. Each simulated wastewater contained 50 ppm of pollutant with 125 ppm of supporting electrolyte (Na_2SO_4). The anode area was 9 cm^2, and a copper plate with a same size acted as cathode. Electromagnetic stirring speed was 300 rpm. The variation of ARG concentration was measured by a UV-vis spectrometer (Agilent 8453). Phenol degradation samples were analyzed by gas chromatography-mass spectrometry (GC-MS, Thermo Fisher). Solid-phase micro-extraction (SPME) was adopted. The rest of the GC-MS details followed the previous report [11]. Non-purgeable organic carbon (NPOC) of maleic acid degradation samples was analyzed by a TOC analyzer (Vario TOC, Elementar). The anode lifetime was regarded as the duration time before the cell voltage reached to 10 V in the accelerated lifetime test (anode area: 2 cm^2, anodic current: 1 A, in 0.5 mol/L Na_2SO_4 solution). During this lifetime test, the Pb^{2+} concentration in the solution was monitored by ICP-AES (iCAP-6000, Thermo).

The embedded hairs changed the morphology of PbO_2 coating (Figs. 1a and b), introducing considerable cracks and making the coating discontinuous. The average size of PbO_2 pyramids became smaller, indicating hairs may inhibit the crystallization process of PbO_2. The increased hairs could further flatten the PbO_2 pyramids (on PbO_2(H10)). Hairs brought massive carbon atoms (Fig. 1c). The embedded hairs were disordered (Figs. 1d and e). The stretching-length of embedded hairs was about 500 μm and their average altitude above the PbO_2 coating plane was about 300 μm (Fig. 1e).

The XRD patterns (Fig. 1f) illustrate an obvious PbO_2 crystal structure variation caused by hairs. Despite of (101) facet and (301) facet, all other peaks' intensities were significantly reduced on PbO_2(H5) and PbO_2(H10). From the calculations on (110) peak, we can find the grain size of PbO_2 was reduced from original 25.3 nm to 21.5 nm when 5 mg/cm^2 of hairs were embedded. Nevertheless, further increase of hairs (10 mg/cm^2) had inconspicuous effect on the gain size. The preferential crystallographic orientation also changed. The (110) facet and (200) facet were no longer the prior exposure facets on PbO_2(H5) and PbO_2(H10). Only (211) facet was the main exposure facet on these hair-embedded electrodes. The above results indicate that even a small amount of hairs could have strong and multiple impacts on the PbO_2 electrodeposition process.

The hydrophobicity of the electrode was also changed by the hairs. The contact angles of water and phenol were 96.4° and 93.8°, respectively, on the unmodified PbO_2 (Fig. 1g). On PbO_2(H5), the angles rose to 118.9° and 94.8° correspondingly. The increasement of hairs would furtherly increase these contact angles (on PbO_2(H10)).

The modifications of the morphology, structure and composition of the electrode surface would lead to the change of electrochemical properties of the electrode. Electrochemical roughness factor (*Rf*) and voltammetric charge (q^*) are two indicators that could reflect the amount and distribution of active sites [28,29], which are calculated from the narrow cyclic voltammograms (Fig. S1 in Supporting information). The roughness factor of PbO_2 was only 723, while that of PbO_2(H5) and PbO_2(H10) were 2695 and 794, respectively (Fig. 2a). The total voltammetric charge (q_T, corresponding to potential scan rate of 5 mV/s in this study) of PbO_2 was only 39.8 mC/cm^2, while that of PbO_2(H5) and PbO_2(H10) were 152.8 mC/cm^2 and 104.7 mC/cm^2, respectively (Fig. 2a). When the potential scan rate increased, the voltammetric charge decreased sharply. The increased amount of total active sites may

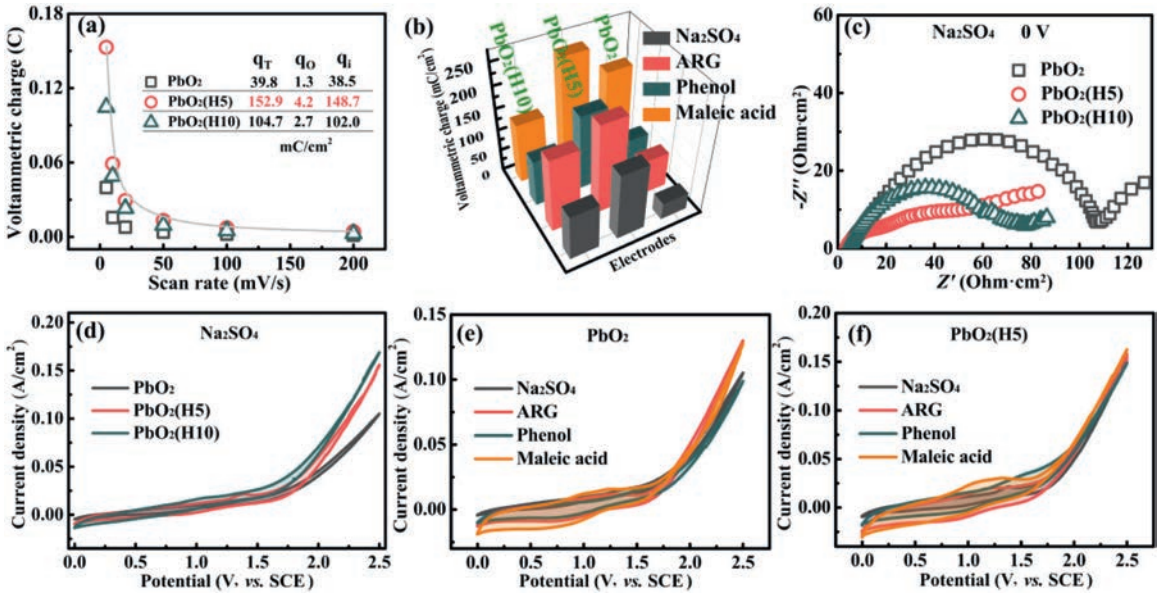

Fig. 2. Electrochemical properties of the electrodes: (a) Voltammetric charge under different potential scan rate (potential range from 0 V to 0.3 V (*vs.* SCE)); (b) Voltammetric charge under scan rate of 5 mV/s in 0.5 mol/L Na_2SO_4 solution containing 2000 ppm of different target pollutant (potential range from 0 V to 0.3 V (*vs.* SCE)); (c) Nyquist plot in in 0.5 mol/L Na_2SO_4 solution (equilibrium potential: 0 V (*vs.* SCE)); (d) Cyclic voltammograms of three electrodes in 0.5 mol/L Na_2SO_4 solution (scan rate: 10 mV/s); Cyclic voltammograms of unmodified PbO_2 (e) and PbO_2(H5) (f) in 0.5 mol/L Na_2SO_4 solution containing 2000 ppm of different target pollutants (scan rate: 10 mV/s).

result from the decrease of grain size and increase of more active facet (Fig. 1f, XRD patterns). But almost all the increased active sites were not the easily accessible active sites (corresponding to the outer voltammetric charge q_o obtained at potential scan rate of 200 mV/s in this study), but were the less accessible active sites (corresponding to the inner voltammetric charge q_i, $q_i = q_T - q_o$). Therefore, it can be deduced that the coating cracks caused by the hairs were another factor that influence the amount and distribution of active sites. It is unnecessary to embed excessive hairs, because hairs are non-conductive obstacles lying on the electrode surface and thereby decrease the effective electroactive sites (like PbO_2(H10)).

When adding the target pollutant in the above narrow CV test, the variation of q^* value could reflect the interaction between the active sites and the pollutant. From Fig. 2b it can been that the hairs enhanced the interaction of all investigated compounds and the PbO_2, especially for ARG and phenol. However, embedding excessive hairs would decrease this effect, especially for maleic acid, indicating the barrier attribution of hairs would neutralize their positive effect of increasing and activating PbO_2 active sites. Appropriate hairs would also decrease the electrode's electrochemical impedance, especially the charge transfer impedance (the high frequency region, Fig. 2c). Excessive hairs would decrease this positive effect, but the diffusion impedance (the low frequency region) would be further decreased. Fig. 2d shows the orientations of hairs on the electrode surface.

The regular CV curves (potential range: 0 – 2.5 V (*vs.* SCE)) obtained in different media could reflect the electrocatalytic activities of the electrodes. From the enhanced response current at high potential (Fig. 2e), it could be found that the hairs would enhance the oxygen evolution reaction (OER) activity of the electrode. The onset oxygen evolution potential remained at ~1.75 V (*vs.* SCE), indicating the change of morphology and PbO_2 crystal structure caused by hairs mainly improved the electron transfer and the mass transfer, while the activation energy of OER was not changed. When pollutants were added (Figs. 2e and f, Fig. S2 in Supporting information), it can be found the oxidation peak and reduction peak between 0.7 V and 1.5 V (*vs.* SCE) emerged, indicating the direct oxidation and reduction of pollutants on the electrode surface were reinforced. The peaks on PbO_2(H5) were more obvious, especially for phenol, indicating appropriate amount of hairs would maximumly increase and activate PbO_2 active sites, especially for the interaction with phenol, which was in good accordance with the narrow CV curves. Excessive hairs would significantly lower the response current at high potential region (OER region) in phenol and maleic acid solution, indicating the electron transfer kinetics from phenol and maleic acid to the electrode surface was slower than OER kinetics for PbO_2(H10).

The efficiency of destroying the azo linkage of ARG was an indicator reflecting the anode's ability of cutting bigger molecules. From Figs. 3a-c it can be seen that PbO_2(H5) exhibited the most competitive results in terms of ARG removal, and this anode's advantage was more obvious under lower current density (*e.g.*, 2 mA/cm^2). However, PbO_2(H10) showed the worst ARG removal efficiency under higher current density, indicating excessive embedded hairs would give negative results. When 10 mmol/L of *tert*-butanol ($^{\bullet}$OH scavenger) was added in the ARG solution (Fig. S3 in Supporting information), the ARG removal efficiencies were enhanced under 20 mA/cm^2 for all electrodes, but which were decreased under lower current densities for hair-embedded electrodes. The former could be attributed to the dominating non-free radical process under higher anodic potential, such as the formation of higher oxide. The latter indicates the important role of free radical route for the hair-embedded electrode under lower anodic potential, which may be one of the reasons for the more advanced performance of PbO_2(H5) under lower current density. The efficiency of destroying phenol ring was another indicator demonstrating the anode's EO ability. From Fig. 3d, it can be seen that although PbO_2(H5) could not compete with PbO_2 on removing phenol under lower current density, but it reversed the situation under higher current density. The embedded hairs also changed the accumulation of intermediate products during phenol degradation (Figs. 3e and f). Compared with PbO_2, PbO_2(H5) inclined to accumulate intermediate products with lower retention time value and lower mass-to-charge ratio, *e.g.*, methanol and hydroxyacetic acid, under higher current density. The result of maleic acid degradation also demonstrated the superiority of hair-embedded electrode in terms of mineralizing small molecular organic acids (especially for

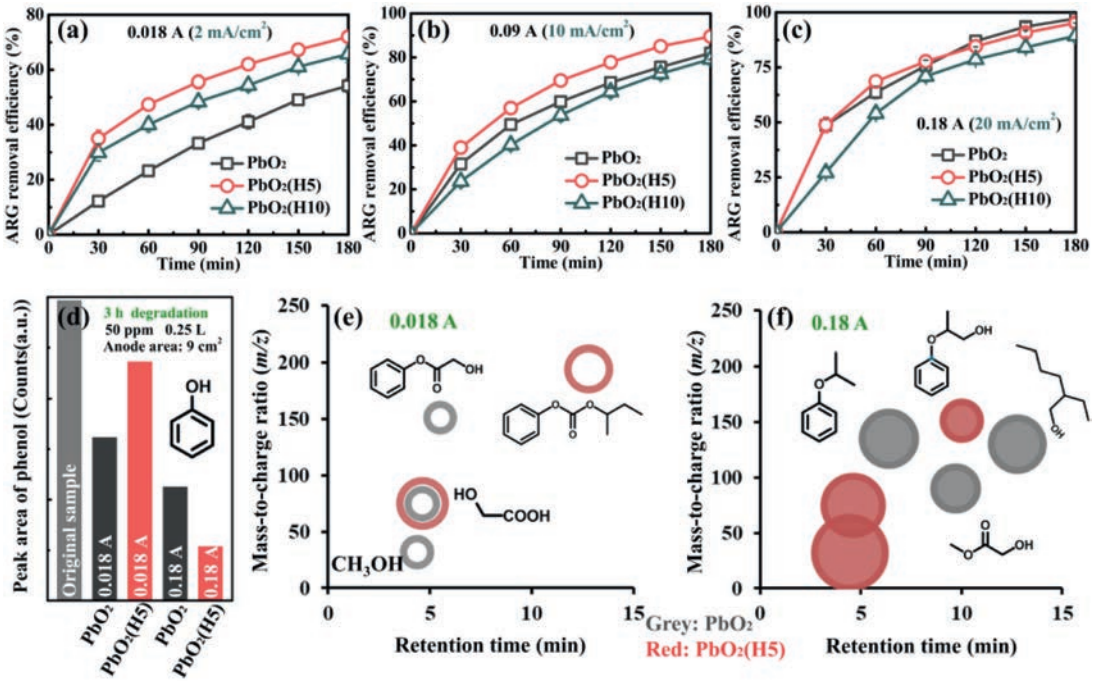

Fig. 3. Electrochemical degradation results: ARG removal efficiency versus time under 0.018 A (a), 0.09 A (b) and 0.18 A (c); (d) Phenol residue after 3 h degradation under 0.018 A and 0.18 A. (e) Mass-to-charge ratio *vs.* retention time about phenol degradation intermediates after 3 h degradation under 0.018 A (gray circle: PbO_2; red circle: PbO_2(H5); circle diameter is proportional to the GC peak area). (f) Mass-to-charge ratio *vs.* retention time about phenol degradation intermediates after 3 h degradation under 0.18 A (All settings of circles are the same as above.).

PbO_2(H5)) under lower current density (Fig. S4 in Supporting information), reflecting by the more obvious decline of NPOC. However, under higher current density, less-volatile intermediate products may accumulate more on hair-embedded electrodes (*e.g.*, hydroxyacetic acid or acetic acid), reflecting by the increase of NPOC.

The hair-embedded electrode also showed their higher stability and safety compared with the unmodified electrode. Fig. S5 (Supporting information) shows that the hair-embedded electrode (PbO_2(H5)) endured ~550 h of harsh electrolysis in the accelerated lifetime test. The cell voltage varied with fluctuations but basically followed the trend of firstly descending (Region I) and then rising (Region II). The descending cell voltage together with the increasing q_T value could be attributed to the electrolyte permeation. The subsequent rising of cell voltage together with the fall back of q_T value suggested the coating loss process, which was confirmed by the images (Fig. S6 in Supporting information) and XRD patterns (Fig. S7 in Supporting information). Some CuO precipitates also formed during this harsh electrolysis process. It is relieved that the released Pb^{2+} ion concentration was acceptable (0.092 ppm), indicating the deactivation of PbO_2(H5) mainly followed the coating detachment mechanism rather than the coating dissolution mechanism. As a result, this hair-embedded PbO_2 could be accepted as a robust and green anode in wide practical applications in the near future. In fact, PbO_2(H5) has been adopted to treat a petrochemical wastewater (major contaminant: caprolactam) at bench scale, which works well so far.

In conclusion, a small amount of embedded hairs could have strong and multiple impacts on the PbO_2 electrodeposition process, changing the PbO_2 morphology and structure, leading to the variation of a variety of electrochemical properties and organic pollutant degradation processes. A modest embedding amount is appropriate, such as PbO_2(H5), which has smaller grain size, larger surface area, lower impedance compared with PbO_2(H10) and unmodified PbO_2. Depending on the type of organic pollutant and current density, PbO_2(H5) exhibits more or less advantages in pollutant combustion or conversion compared with other two electrodes. PbO_2(H5) could also be accepted as a robust and green anode with satisfying overall performance, which may have bright future in small practical wastewater treatment system.

Declaration of competing interest

We declare that we have no financial and personal relationships with other people or organizations that can inappropriately influence our work, there is no professional or other personal interest of any nature or kind in any product, service and/or company that could be construed as influencing the position presented in, or the review of, the manuscript entitled.

Acknowledgments

This study is financed by the National Natural Science Foundation of China (No. 21706153) and Natural Science Basic Research Plan in Shaanxi Province of China (No. 2018JQ2066).

Supplementary materials

Supplementary material associated with this article can be found, in the online version, at doi:10.1016/j.cclet.2021.07.061.

References

[1] L.U.S. Faria, K.S.G.C. Oliveira, A.B. Veroli, J.M. Aquino, L.A.M. Ruotolo, Chem. Eng. J. 418 (2021) 129363.
[2] E. Brillas, C.A. Martinez-Huitle, Appl. Catal. B: Environ. 166 (2015) 603–643.
[3] C.A. Martínez-Huitle, M. Panizza, Curr. Opin. Electrochem. 11 (2018) 62–71.
[4] Y. Liu, G. Gao, C.D. Vecitis, Acc. Chem. Res. 53 (2020) 2892–2902.
[5] Y.B. Liu, F.Q. Liu, N. Ding, et al., Chin. Chem. Lett. 31 (2020) 2539–2548.
[6] Y.F. Guo, Z.C. Xu, S.Y. Guo, et al., Sep. Purif. Technol. 261 (2021) 118304.
[7] G. Hua, X. Zhicheng, Q. Dan, et al., Chemosphere 261 (2020) 128157.
[8] G. Ren, M. Zhou, M. Liu, L. Ma, H. Yang, Chem. Eng. J. 298 (2016) 55–67.
[9] J. Radjenovic, N. Duinslaeger, S.S. Avval, B.P. Chaplin, Environ. Sci. Technol. 54 (2020) 14815–14829.
[10] W. Zheng, Y. Liu, W. Liu, et al., Water Res. 194 (2021) 116961.

[11] X. Zhang, D. Shao, W. Lyu, et al., Chem. Eng. J. 395 (2020) 125145.
[12] J. Lei, Z. Xu, X. Yuan, et al., J. Water Process Eng 36 (2020) 101305.
[13] J.N. Lei, Z.C. Xu, H. Xu, et al., J. Environ. Chem. Eng. 8 (2020) 103773.
[14] D. Shao, Y. Zhang, W. Lyu, et al., J. Hazard. Mater. 390 (2020) 122174.
[15] Y.P. Wang, C.Z. Zhou, J.H. Wu, J.F. Niu, Chin. Chem. Lett. 31 (2020) 2673–2677.
[16] D. Shao, X. Zhang, W. Lyu, et al., ACS Appl. Mater. Interfaces 10 (2018) 44385–44395.
[17] D. Shao, X. Zhang, Z. Wang, et al., Appl. Surf. Sci. 515 (2020) 146003.
[18] D. Shao, W. Lyu, J. Cui, et al., Chemosphere 241 (2020) 125103.
[19] J. Li, Y.J. Li, Z.K. Xiong, G. Yao, B. Lai, Chin. Chem. Lett. 30 (2019) 2139–2146.
[20] R. Xie, X. Meng, P. Sun, et al., Appl. Catal. B: Environ. 203 (2017) 515–525.
[21] Z. Xu, H. Liu, J. Niu, et al., J. Hazard. Mater. 327 (2017) 144–152.
[22] Z. Wang, M. Xu, F. Wang, et al., Electrochim. Acta 247 (2017) 535–547.
[23] Q. Zhuo, Q. Xiang, H. Yi, et al., J. Electroanal. Chem. 801 (2017) 235–243.
[24] X. Duan, C. Zhao, W. Liu, X. Zhao, L. Chang, Electrochim. Acta 240 (2017) 424–436.
[25] R.M. Farinos, L.A.M. Ruotolo, Electrochim. Acta 224 (2017) 32–39.
[26] Q. Dai, J. Zhou, M. Weng, et al., Sep. Purif. Technol. 166 (2016) 109–116.
[27] D. Shao, W. Yan, X.L. Li, H.H. Yang, H. Xu, Ind. Eng. Chem. Res. 53 (2014) 3898–3907.
[28] F. Montilla, E. Morallón, A. De Battisti, J.L. Vázquez, J. Phys. Chem. B 108 (2004) 5036–5043.
[29] S. Asim, Y. Zhu, M. Rana, et al., Chemosphere 169 (2017) 651–659.